Rapid Folding of Calcium-Free Subtilisin by a Stabilized Pro-Domain Mutant†

Biao Ruan, Joel Hoskins, and Philip N. Bryan*

Center for Advanced Research in Biotechnology, University of Maryland Biotechnology Institute, 9600 Gudelsky Drive, Rockville, Maryland 20850

Received February 15, 1999; Revised Manuscript Received May 4, 1999

ABSTRACT: In vitro folding of mature subtilisin is extremely slow. The isolated pro-domain greatly accelerates in vitro folding of subtilisin in a bimolecular reaction whose product is a tight complex between folded subtilisin and folded pro-domain. In our studies of subtilisin, we are trying to answer two basic questions: why does subtilisin fold slowly without the pro-domain and what does the pro-domain do to accelerate the folding rate? To address these general questions, we are trying to characterize all the rate constants governing individual steps in the bimolecular folding reaction of pro-domain with subtilisin. Here, we report the results of a series of in vitro folding experiments using an engineered pro-domain mutant which is independently stable (proR9) and two calcium-free subtilisin mutants. The bimolecular folding reaction of subtilisin and proR9 occurs in two steps: an initial binding of proR9 to unfolded subtilisin, followed by isomerization of the initial complex into the native complex. The central findings are as follows. First, the independently stable proR9 folds subtilisin much faster than the predominantly unfolded wild-type pro-domain. Second, at micromolar concentrations of proR9, the subtilisin folding reaction becomes limited by the rate at which prolines in the unfolded state can isomerize to their native conformation. The simplest mechanism which closely describes the data includes two denatured forms of subtilisin, which form the initial complex with proR9 at the same rate but which isomerize to the fully folded complex at much different rates. In this model, 77% of the subtilisin isomerizes to the native form slowly and the remaining 23% isomerizes more rapidly (1.5 s^{-1}). The slow-folding population may be unfolded subtilisin with the trans form of proline 168, which must isomerize to the cis form during refolding. Third, in the absence of proline isomerization, the rate of subtilisin folding is rapid and at [proR9] ≤ 20 μM is limited by the rate at which the proR9 forms a collision complex with unfolded subtilisin. Without proline isomerization, the rate of the isomerization of the initial collision complex to the folded complex is >3 s^{-1}. The implications of these results concerning why subtilisin folds slowly without the pro-domain are discussed.

Subtilisin BPN′ is an extracellular serine proteinase from *Bacillus amyloliquefaciens*. It is produced in vivo from a pre-pro-protein (*1*, *2*). The 30 amino acid presequence serves as a signal peptide for protein secretion across the membrane and is hydrolyzed by a signal peptidase (*3*). The extracellular part of the maturation process involves folding of prosubtilisin, self-processing of the 77 amino acid pro-domain to produce a processed complex, and finally degradation of the pro-domain to create the 275 amino acid mature form of the enzyme (*4*, *5*). In vitro folding of mature subtilisin is extremely slow (*6*). The isolated pro-domain greatly accelerates the in vitro folding of subtilisin in a bimolecular reaction whose product is a tight complex between folded subtilisin and folded pro-domain (*7*). In the complex, the 77 amino acid pro-domain has a compact structure with a four-stranded β-sheet and two three-turn α-helices (*8*). The interaction of the pro-domain with subtilisin is believed to hasten the folding process by providing an energetically more favorable folding pathway (*9*). This phenomenon has general similarity to the folding of α-lytic protease, which is catalyzed by a 166 amino acid pro-domain (*10*, *11*). Both subtilisin and α-lytic protease are extracellular, bacterial, serine proteinases, though they are not evolutionarily related. Several other proteinases also have been found to rely on their pro-segment to achieve their native folds. These include aspartic proteinases, such as carboxypeptidase Y (*12*), Yapsin 1 (*13*), and protease A (*14*), cysteine proteinases such as Cathepsin D and Papain (*15*), and pro-hormone convertases (*16*).

In vitro folding of proteins the size of subtilisin freqently occurs within seconds, and apart from aggregation of unfolded states, impediments to protein folding are not well understood. Thus, in our studies of subtilisin, we are trying to answer two basic questions: why does subtilisin fold slowly without the pro-domain and what does the pro-domain do to accelerate the folding rate? To address these general questions, we are trying to characterize all the rate constants governing individual steps in the bimolecular reaction of pro-domain with unfolded subtilisin. Previous results from our laboratory can be summarized as follows. (1) Inactive subtilisin mutants with a deletion of the calcium-binding loop are thermodynamically stable but fold very slowly (k_{fold} < 0.1 h^{-1} in 30 mM Tris-HCl,[1] pH 7.5, at 25 °C) (*6*). (2) The

† This work was supported by NIH Grant GM42560.

* To whom correspondence should be addressed. Phone: 301-738-6220. Fax: 301-738-6255. E-mail: bryan@umbi.umd.edu.

10.1021/bi990362n CCC: $18.00
Published on Web 06/09/1999

isolated pro-domain is largely unfolded ($\Delta G_{folding} = 2$ kcal/mol in 30 mM Tris-HCl, pH 7.5 at 25 °C) but catalyzes the folding of calcium-free subtilisin at a rate of 500 M^{-1} s^{-1} (*7*, *9*). (3) The pro-domain appears to accelerate subtilisin folding by stabilizing a nativelike intermediate state (*17*). (4) As stabilizing mutations are introduced into the pro-domain, the folding reaction with subtilisin becomes faster but distinctly biphasic (*18*, *19*).

A minimal reaction mechanism for the bimolecular folding of subtilisin is as follows:

$$P + S_u \rightleftarrows PS_I \rightleftarrows PS$$

where S_u is unfolded subtilisin, P is pro-domain, PS_I is an intermediate complex which accumulates in the course of the reaction, and PS is the fully folded complex. Here we report the results of a series of kinetic experiments using a pro-domain mutant denoted proR9, which has been engineered to be independently stable, and two inactive, calcium-free subtilisin mutants. By using the stable proR9 instead of wild-type pro-domain, we are able to accelerate the initial binding step to the point that isomerization of PS_I to PS becomes rate limiting in the folding reaction. This allowed us to examine the nature of the isomerization step in detail.

MATERIALS AND METHODS

Mutagenesis and Cloning of proR9. Mutagenesis and protein expression of pro-domain mutants were performed using vector called pJ1. Vector pJ1 is identical to pG5 (*20*) except that the *Cla*I site of pG5 has been removed. The pro-domain gene for proR1 was inserted between *Nde*I and *Hin*dIII sites in the polycloning site of pJ1. When superinfected with helper phage M13K07, the M13 origin enables the DNA replication in single-stranded form for mutagenesis and sequencing. Mutagenesis of the cloned pro-domain gene was performed according to the oligonucleotide-directed in vitro mutagenesis system, version 2, Sculptor system (Amersham International plc) or Kunkel dUTP incorporation method (Kunkel, 1985; Kunkel et al., 1987). *Escherichia coli* TG1 [K12, Δ(*lac-pro*), *sup*E, *thi*, *hsdD5*/F'traD36, *pro*A^+B^+, *lacI*^{q}, *lacZ*Δ*M*15] was obtained from the oligonucleotide-directed in vitro mutagenesis system version 2 (Amersham International plc). Competent *E. coli* TG1 cells were transformed with mutagenesis product, and single-stranded phagemid DNA was then prepared from TG1 cells superinfected with helper phage, while double-stranded phagemid DNA was isolated using Wizard Plus Minipreps DNA Purification System. Phagemid DNA was sequenced as described in Sequenase Protocol (U.S. Biochemical), using either single-stranded or double-stranded phagemid DNA. Upon confirmation of the mutations, the mutant double-stranded phagemid DNA was used to transform the *E. coli* production strain, BL21(DE3)[F^-, *hsdS*, *gal*] (*21*). BL21-(DE3) cells contain the bacteriophage T7 gene 10 which encodes the bacteriophage T7 RNA polymerase. Gene 10 is under the control of *lac* UV5 promoter, inducible by IPTG.

Fermentation and Purification of proR9. The transformed production strain BL21(DE3) was plated out on selection plates. Ten milliliters of LB broth (10 g of tryptone, 5 g of yeast extract, and 10 g of NaCl/L media) supplemented with 100 μg/mL ampicillin was inoculated with 4−6 ampicillin-resistant colonies in a 250 mL baffled flask. The culture was grown at 37 °C, 300 rpm, until mid log phase. This culture was used to inoculate 1.5 L of LB Broth buffered with 2.3 g of KH_2PO_4 and 12.5 g of K_2HPO_4/L media supplemented with 100 μg/mL ampicillin. The culture was grown at 37 °C in a BioFlo Model C30 fermenter (New Brunswick Scientific Co., Inc.) until an A_{600} 1−1.2 was attained, upon which 1 mM IPTG was added to induce the production of T7 RNA polymerase that directs synthesis of target DNA message. Three hours after induction, the cells were harvested by centrifugation for 30 min at 4 °C, 10 000 rpm in a J2-21 centrifuge (Beckman Instruments) with a JA-14 rotor.

ProR9 was purified using a freeze−thaw method to release soluble protein form the cells (*22*). *E. coli* paste from a 1.5 L fermentation (∼5 g) was suspended in 10 mL of cold phosphate-buffered saline (PBS) and 20 mL of water. PMSF was added to final concentration of 1 mM, DNase I to 10 μg/mL, and the oxidized form of glutathione (100 mg in 1 mL total volume of 100 mM KP_i, pH 7.0) to 1.6 mg/mL. The resuspension was frozen by submerging in a dry ice/ethanol bath until it was completely frozen, and then thawed in a room-temperature water bath. This cycle was repeated two additional times, with addition of 100 μL of Glutathione stock solution before each cycle. The final mixture was centrifuged at 4 °C for 10 min at 10 000 rpm in a J2-21 centrifuge (Beckman Instruments) with a JA-14 rotor. The supernatant containing the soluble protein was diluted 4-fold with 20 mM Hepes, pH 7.0, and further purified as described (*7*).

A 1.5 L fermentation yielded 60−70 mg of purified proR9. The concentration of proR9 was determined by UV absorbance using 1 mg/mL = A_{275} of 0.67.

Fermentation and Purification of Subtilisin Mutant Sbt70. The gene for sbt70 was subcloned into PJ1 vector (denoted pJ12) and transformed into *E. coli* production strain BL21-(DE3). Fermentation and expression steps for sbt70 are essentially the same as for proR9. *E. coli* paste from a 1.5 L fermentation (∼5 g) was resuspended in 50 mL of lysis buffer (50 mM Tris-HCl, pH 8.0/100 mM NaCl/1 mM EDTA) and PMSF was added to a final concentration of 1 mM and DNase I (in 40 mM Tris-HCl and 1 M $MgCl_2$) to 20 μg/mL. The cells were lysed by two passes through a French Press, and additional DNase I was added to a final concentration of 25 μg/mL. Inclusion bodies containing mutant proteins were recovered by centrifugation at 10 000 g, 4 °C with a JA-17 rotor for 20 min in a Beckman J2-21 centrifuge. The resulting pellet was washed three times by repeated resuspension in 60 mL of ice-cold 20 mM Hepes, pH 7.0, and centrifugation for 10 min at the same condition as above. The final pellet was then resuspended in 50 mL of ice-cold 20 mM Hepes, pH 7.0, containing 2 M urea (freshly dissolved), frozen on dry ice, and allowed to thaw at room temperature to clarify the solution. In one preparation, in which a precipitate formed, the volume was increased by 10 mL, and the freeze/thaw cycle was repeated. The

[1] Abbreviations: P_i, phosphate; proWT, wild-type pro-domain of subtilisin BPN′; proR9, subtilisin BPN′ pro-domain with the following mutations: substitution of amino acids 17−21 (TMSTM) with SGIK and the substitutions A23C, K27E, V37L, Q40C, H72K, H75K; Sbt15, subtilisin BPN′ with the mutations deletion of amino acids 75−83 (Δ75−83), Y217K, N218S, and S221C; Sbt70, subtilisin BPN′ with the mutations K43N, M50F, A73L, Δ75−83, Q206V, Y217K, N218S, and S221A; Tris, Tris(hydroxymethyl)aminomethane;

solution then was centrifuged for 10 min, and the supernatant applied to a Productive DE cartridge (Metachem Technologies Inc.) equilibrated with 20 mM Hepes, pH 7.0/2 M urea. The cartridge was washed with 40 mL of cold 20 mM Hepes, pH 7.0/2 M urea. Flow through and wash fractions were combined and dialyzed 36−48 h at room temperature against 3.5 L of 100 mM KP_i, pH 7.0 to fold the sbt70.

An affinity agarose column was prepared by coupling the tetra-peptide A-L-A-L (Sigma) to Affi-Gel 10 (Bio-Rad) following the manufacturer's protocol. The DE cartridge-purified protein was split and each half loaded onto a 4.5 mL column of A-L-A-L-agarose equilibrated with 20 mM Hepes, pH 7.0. The column was washed with 20 mL of 20 mM Hepes, pH 7.0/1 M NaCl followed by 10 mL of 20 mM Hepes, pH 7.0, and the protein was eluted with 50 mM of triethylamine, pH 11.1. Peak fractions (1 mL each) of the protein were immediately neutralized by the addition of 0.1 mL of 1 M KP_i, pH 7.0, and pooled together, then dialyzed overnight against 3.5 L of 2 mM ammonium carbonate. A 1.5 L fermentation yielded ~100 mg of purified sbt70. Purified protein was lyophilized and stored at −20 °C. The concentration of sbt70 was determined by UV absorbance using 1 mg/mL = A_{280} of 1.12.

Fermentation and Purification of Sbt15. The Sbt15 gene has been cloned into a pUB110-based plasmid expression vector and transformed into *Bacillus subtillis* (*6*). The *B. subtilis* strain used as the host contains a chromosomal deletion of its subtilisin gene and therefore produces no background wild-type activity. The seed was grown in LB broth supplemented with 10 μg/mL Kan in a 1.5 L BioFlo model C30 fermenter (New Brunswick Scientific Co., Inc.) at pH 7.55, 34 °C, 800 rpm for 16 h. The supernatant of the culture contains the secreted sbt15 protein. Ice-cold acetone was added to the supernatant to a 40% concentration (vol/vol). The mixture was centrifuged for 30 min at 4 °C, 6000*g* in a J2-21 centrifuge (Beckman Instruments). Additional ice-cold acetone was added to the supernatant to achieve a total acetone concentration of 70% (vol/vol). The mixture was centrifuged again, and the precipitate was resuspended in 20 mM Hepes, pH 7.0. The solution was centrifuged again to get rid of undissolved precipitate. The resulting supernatant was then purified to homogeneity by anion-exchange chromatography using DE52, and the peak fractions were checked on SDS−polyacrymide (SDS−PAGE) gels (Novex Experimental Technoolgy). The desired fractions were pooled and dialyzed against 2 mM ammonium bicarbonate, pH 7.0, at 4 °C. A 1.5 L fermentation yielded ~200 mg of purified sbt15. After lyophilization, the protein sample was stored at −20 °C. The concentration of sbt15 was determined by UV absorbance using 1 mg/mL = A_{280} of 1.12.

Kinetics of Pro-Domain Binding to Native Sbt70. The rate of binding of the proR9 to folded Sbt70 was monitored by fluorescence (excitation λ = 300 nm, emission λ, 340 nm cutoff filter) using a KinTek Stopped-Flow model SF2001. The reaction was followed by the 1.2-fold increase in the tryptophan fluorescence of Sbt70 upon its binding of the pro-domain (*7*). Pro-domain solutions of 10−160 μM in 30 mM Tris-HCl, and 5 mM KP_i, pH 7.5, were mixed with an equal volume of 2 μM subtilisin, 30 mM Tris-HCl, and 5 mM KP_i, pH 7.5, in a single mixing step. Typically 10−15 kinetic traces were collected for each [P]. Final [Sbt70] was 1 μM and final [P] were 5−80 μM.

Kinetic Analysis of Pro-Domain Facilitated Subtilisin Folding. Single Mixing. Refolding of subtilisin is accompanied by a 1.5-fold increase in the tryptophan fluorescence of subtilisin upon folding into its complex with the pro-domain. There are three tryptophan residues in the subtilisin mutants and none in proR9. Reaction kinetics were measured using a KinTek Stopped-Flow model SF2001 (excitation λ = 300 nm, emission = 340 nm cutoff filter) as described (*9*). A stock solution of subtilisin at a concentration of 100 μM in 100 mM KP_i, pH 7.0, was prepared for refolding studies. Subtilisin was denatured by diluting 20 μL of the stock solution into 1 mL of 50 mM HCl. The samples were neutralized by mixing the subtilisin and HCl solution into an equal volume of 60 mM Tris-base, pH 9.4, KP_i, and pro-domain in the KinTek Stopped-flow (final buffer concentrations were 30 mM Tris-HCl, and 5 mM KP_i, pH 7.5). Although the final concentration of subtilisin was 1 μM in most experiments, it could be varied from 0.1 to 10 μM without affecting the kinetics of folding under conditions of pro-domain excess. When using 1 μM subtilisin, the pro-domain concentration was varied from 5 to 20 μM. Typically 10−15 kinetic traces were collected for each [P].

Double Jump: Renaturation−Denaturation. The kinetics of the formation of the folded complex, PS, were determined by a double-jump renaturation−denaturation experiment. The KinTek Stopped Flow in the three syringe configuration was used to perform the two mixing steps. In the first mixing step, 3 μM subtilisin in 50 mM HCl is mixed with a variable concentration of pro-domain in 60 mM Tris-base and KP_i. The resulting solution is 30 mM Tris-HCl and 5 mM Kpi, pH 7.5. The final concentration of subtilisin was 1.5 μM, while the pro-domain concentration was varied from 5 to 20 μM after the first mixing step. Subtilisin and pro-domain are allowed to fold under native conditions in the delay line of the stopped-flow instrument for aging times ranging 0.5−60 s. After the prescribed aging time, the subtilisin-pro-domain solution is mixed 2:1 with 0.1 M H_3PO_4 to bring the pH to 2.3. Fluorescence data for the denaturation of folded complex was collected after the second mixing step. At each renaturation time point, the denaturation curve was fit to a single exponential decay curve. The amplitude of the decay curve was recorded as a function of refolding time to assess the amount of folded complex which had accumulated at each renaturation time. Typically 10−15 kinetic traces were collected for each renaturation time point.

Double Jump: Denaturation−Renaturation. A double jump denaturation−renaturation experiment was used to study the effect of denaturation time on the rates and amplitudes of the folding reaction. The KinTek Stopped Flow in the three syringe configuration was used to perform the two mixing steps. In the first mixing reaction, 3 μM of subtilisin and 30 μM proR9 in 0.05 M KP_i, pH 7.2 was denatured by mixing with an equal volume of 0.1 M phosphoric acid. The resulting solution has a pH of 2.15. The denaturation reaction was aged for varied lengths of time and then mixed with one-half volume of 0.15 M KPO_4, pH 12.0. The final conditions were 1 μM of sbt15 and 10 μM of proR9 in 0.1 M KP_i, pH 7.2, at 25 °C. The folding process is then followed by fluorescence change.

A second double mixing denaturation−renaturation experiment was used to follow folding kinetics after 0.5 s of denaturation. The two mixing steps were performed using a

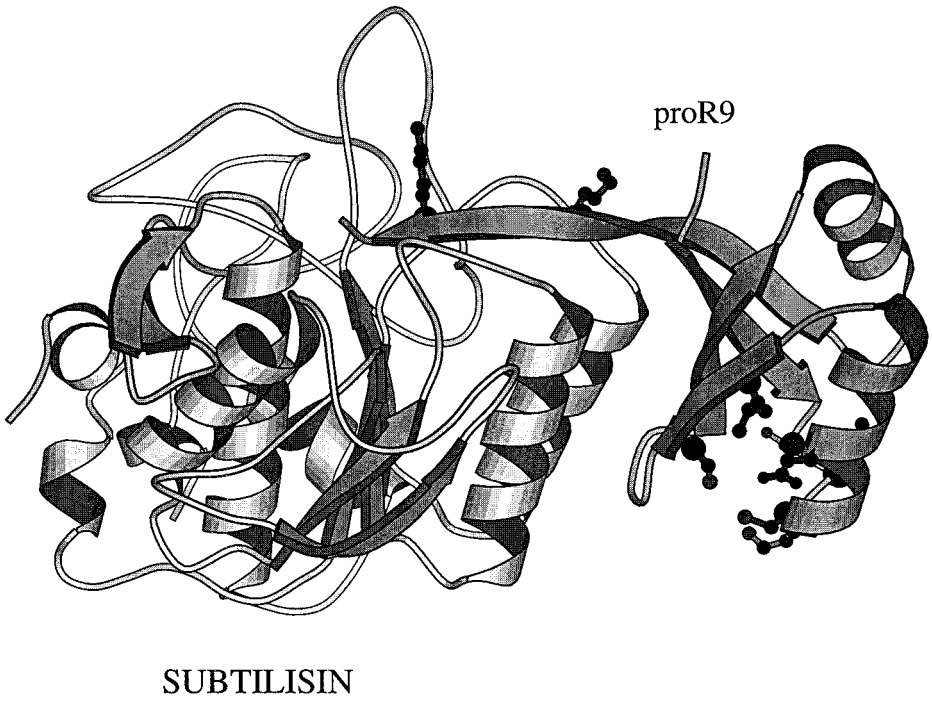

FIGURE 1: Structure of the pro-domain in complex with Sbt70. Drawing depicting the α-carbon backbone of the bimolecular complex of subtilisin Sbt70 (lighter shading) and proR9 (darker shading). The positions of mutant side chains in proR9 are shown as balls and sticks. Drawn with MOLSCRIPT (*38*).

BioLogic SFM-4 Q/S in the stopped flow mode. In the first step, 2 μM Sbt70 in 10 mM KP_i, pH 7.2, is mixed with an equal volume of 100 mM HCl. The resulting solution is 1 μM Sbt70, 50 mM HCl, and 5 mM KP_i, pH 2.1. After 0.5 s, the denatured sbt70 solution is mixed with an equal volume of 60 mM Tris-base, 5 mM KP_i, and variable amounts of proR9. The resulting solution is 0.5 μM Sbt70, 5−20 μM proR9, 30 mM Tris-HCl, and 5 mM Kpi, pH 7.5. The renaturation process is followed by fluorescence change.

Triple Jump: Denaturation−Renaturation−Denaturation. A triple mixing denaturation−renaturation−denaturation experiment was used to measure directly the accumulation of native complex after a denaturation time of 0.5 s. The three mixing steps were performed using a BioLogic SFM-4 Q/S in the stopped flow mode. In the first step, 5 μM Sbt70 in 10 mM KP_i, pH 7.2, is mixed with an equal volume of 100 mM HCl. The resulting solution is 2.5 μM Sbt70, 50 mM HCl, 5 mM KP_i, pH 2.1. After 0.5 s, the denatured sbt70 solution is mixed with an equal volume of 60 mM Tris-base, 5 mM KP_i, and 10 μM proR9. The resulting solution is 1.25 μM Sbt70, 5 μM proR9, 30 mM Tris-HCl, 5 mM Kpi, pH 7.5. Sbt70 and proR9 are allowed to fold under native conditions in the delay line for aging times ranging 0.5−60 s. After the prescribed aging time, the Sbt70-proR9 solution is mixed 3:1 with 0.132 M H_3PO_4 to bring the pH to 2.3 and denature the folding reaction. At each renaturation time point, the denaturation curve was fit to a single-exponential decay curve. The amplitude of the decay curve was recorded as a function of refolding time to assess the amount of folded complex which had accumulated at each renaturation time.

Data Analysis. Fitting to single or double exponential kinetic equations or to binding equations was done using KaleidaGraph Software, version 3.0 (Abelbeck Software). More complicated kinetic mechanisms were simulated using KinTekSim Freeware (*23*, *24*), which was obtained from the KinTek Corporation website (www.kintek-corp.com).

RESULTS

Selection and Engineering of proR9. In complex with subtilisin, the pro-domain folds into a stable compact structure comprising a four-stranded antiparallel β-sheet and two three-turn α-helices (Figure 1). When isolated from subtilisin, the pro-domain is 97% unfolded even under optimal folding conditions (*9*). To simplify the kinetic studies as much as possible, we wished to create a pro-domain which would be stably folded when isolated from subtilisin. To stabilize the pro-domain, four mutations were identified using phage-display selection as described in detail in Ruan et al. (*25*). These four mutations (A23C, K27E, V37L, and Q40C) increased stability by 6 kcal/mol from $\Delta G_{folding} = 2$ kcal/mol for proWT to −4 kcal/mol for the phage-selected mutant, denoted proR1 (*25*). Unfortunately, stabilized pro-domain mutants, including ProR1, were found to have an appreciable tendency to form an adventitious dimer (*18*, *19*, *25*). Since dimerization complicates kinetic analysis of pro-domain-assisted subtilisin folding, we designed two further modifications to try to eliminate dimerization without otherwise affecting the ability of the pro-domain to interact with subtilisin. The X-ray crystallographic structure of the complex of the pro-domain with subtilisin suggested two regions of the pro-domain which might create an interface for dimerization. First, the five amino acid loop between the β1 strand and α-helix 1 (T17, M18, S19, T20, and M21) is partially disordered in the complex, and the two methionine residues protrude into the solvent. Second, the C-terminal amino acids (H75, V74, A73,H72, A76, and Y77) are expected to be disordered in the isolated pro-domain since all of their contacts are with the subtilisin active site (*8*). To

try to eliminate these potential dimer interfaces T17, M18, S19, T20, and M21 were replaced by the amino acid residues SGIK to remove the exposed methionines. H72 and H75 were mutated to Lys to increase electrostatic repulsion in the C-terminal region. The resulting pro-domain mutant is named proR9. Although it is not known which of the two regions was responsible for the adventitous dimerization, the dissociation constant for dimerization of proR9, as determined by sedimentation equilibrium, is very weak (K_d = 0.5 mM in 0.1 M KP_i, pH 7.0, 25 °C). $\Delta G_{folding}$, as determined by differential scanning calorimetry, was the same as for proR1 [−4 kcal/mol (0.1 M KP_i, pH 7.0, 25 °C]. All kinetic experiments in this paper were carried out using proR9.

Subtilisin Engineered for Facile Folding. Mature subtilisin BPN′, once denatured, refolds to the native state very slowly ($\tau >$ weeks) in the absence of the pro-domain. Even when catalyzed by the isolated pro-domain in a bimolecular reaction, refolding of subtilisin occurs at a rate of only ∼0.2 s^{-1} M^{-1} of pro-domain (*26*). The slow time scale of in vitro folding makes detailed kinetic analysis of the process problematic. To make the study of subtilisin folding more tractable, we have engineered subtilisin mutants for facile folding (*27*). A major part of the kinetic barrier to folding subtilisin involves formation of a high-affinity calcium-binding site ($K_a = 10^7$ M^{-1} at 25 °C), called site A (*6*). Deletion of amino acids 75−83 removes the calcium A-site and destabilizes subtilisin but greatly accelerates both uncatalyzed folding (*6*) and pro-domain catalyzed folding (*7*). Both subtilisin mutants used in these studies have amino acids 75−83 deleted. Mutant Sbt15 also contains the mutation of the active-site serine 221 to cysteine, which decreases peptidase activity by ∼50000-fold, and three other substitutions M50F, Y127K, and N218S to help restore stability lost due to the calcium loop deletion (*7*). Mutant Sbt70 contains the mutation S221A, which decreases peptidase activity by $\sim 10^6$-fold and six stabilizing substitutions (K43N, M50F, A73L, Δ75−83, Q206V, Y217K, and N218S) (*9*). None of the mutant amino acids except residue 221 contact the pro-domain in the bimolecular complex (*8*). The catalyzed folding of sbt15 and sbt70 with proR9 were compared to determine whether different amino acids at position 221 would affect the kinetics of the reaction. The folding of both turned out to be similar in most respects, although a difference in the rate of denaturation at pH 2.1 (k_{unfold} = 0.47 s^{-1} for sbt15 vs k_{unfold} = 30 s^{-1} for sbt70) was exploited in studying the effect of denaturation time on refolding kinetics, as described later.

Analysis of Pro-Domain proR9 Binding to Native Subtilisin sbt15. To verify that proR9 interacts with native subtilisin in the manner predicted by its increased stability, kinetic and equilibrium binding experiments were carried out. It was shown previously that increasing the stability of pro-domain by introducing stabilizing mutations in regions of the pro-domain, which do not directly contact subtilisin, increased its binding constant for subtilisin (*19*, *25*). Binding approaches its maximum as the fraction of folded pro-domain increases to 1.

Kinetics of Binding. The rate of proR9 binding to subtilisin was measured using typtophan fluorescence. Tryptophan fluorescence at 345 nm increases by around 1.2-fold upon binding of the pro-domain to folded sbt15. The rate constant for binding, k_{obs}, was determined by measuring the rate of the fluorescence changes at different proR9 concentrations. The binding reaction was carried out in 30 mM Tris-HCl and 5 mM KP_i, pH 7.5, with excess amount of pro-domain. Pseudo-first-order kinetics were observed in all the binding reactions. A plot of k_{obs} versus [proR9] is linear up to 40 μM proR9 with a slope of 1.23×10^6 M^{-1} s^{-1}. This rate of binding is slightly higher than observed for proWT (8×10^5 M^{-1} s^{-1}).

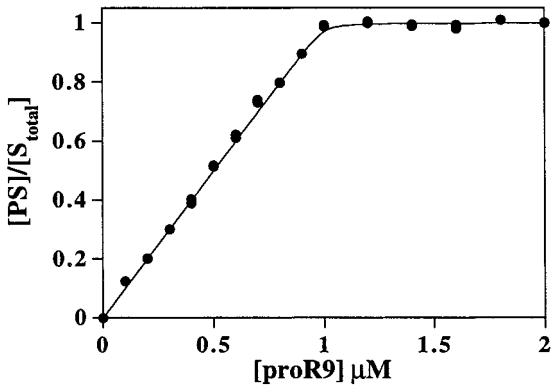

FIGURE 2: Determination of the dissociation constant for proR9 and sbt15. The fluorescence increase upon binding proR9 to 1 μM of folded sbt15 was used to calculate the amount of proR9-sbt15 complex versus the total proR9 concentration. The data were fit to eq 1 in the text to determine that the dissociation constant is ≤1 nM.

Equilibrium Binding. The dissociation constant of proR9 and sbt15 was measured in experiments that determine the fluorescence increase upon proR9 binding to sbt15. Varied amounts of proR9 were mixed with 1 μM of folded sbt15, and the fluorescence was measured. The fraction of sbt15−proR9 complex, calculated from fluorescence change, versus concentration of proR9 is plotted in Figure 2. To determine a binding constant, the quadratic formula was used to solve the binding equation for fraction bound:

$$[PS]/[S_{total}] = ([P_{total}] + [S_{total}] + K_d - (([P_{total}] + [S_{total}] + K_d)^2 - 4[P_{total}][S_{total}])^{1/2})/2[S_{total}]$$

The data in Figure 2 were fit using K_d = 1 nM, which can be considered an upper limit. This K_d is consistent with the expectation that the fully folded proR9 would bind significantly tighter than proWT, which has a K_d for sbt15 of ∼10 nM.

Transient State Kinetic Analysis of proR9 Catalyzed Subtilisin Folding. Measuring the Rate of the Binding Phase. In the single mixing experiments, denatured subtilisin sbt15 was refolded with an excess of proR9 in the stopped flow fluorimeter. The rates and amplitudes of fluorescence changes during a single turnover of subtilisin folding were measured. ProR9 does not have tryptophan residues, and therefore, the fluorescence increase observed above 345 nm upon excitation at 300 nm is due solely to the conversion of denatured subtilisin to the partially folded intermediate complex and the final native complex. The folding reaction was carried out at 30 mM Tris and 5 mM KP_i, pH 7.5 at 25 °C, taking advantage of the fact that uncatalyzed folding of sbt15 is very slow under low ionic strength conditions (<0.1 h^{-1}). The folding reaction was followed using 1 μM denatured sbt15 and varied proR9 concentrations. The folding reaction

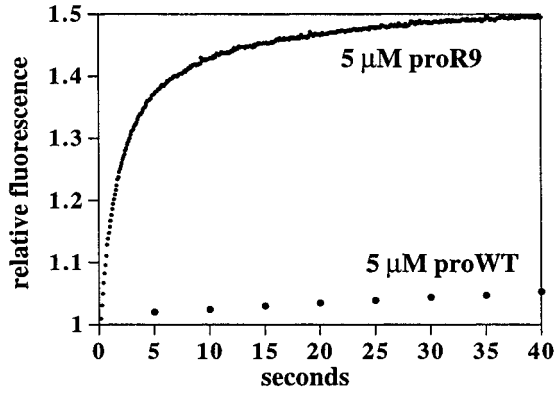

FIGURE 3: Folding rate of Sbt70 in the presence of the proWT and proR9. pro WT or proR9 (5 μM) and 1 μM denatured Sbt70 were mixed in 5 mM KPO4, 30 mM Tris, pH 7.5, at 25 °C. The reaction was followed by the increase in tryptophan fluorescence which occurs upon folding of subtilisin into the pro-domain subtilisin complex.

is much faster than that observed with proWT and distinctly biphasic (Figure 3). The biphasic kinetics nature suggested that intermediate species are populated in the course of the folding (*28*). The folding curves were fit to a double exponential equation and the rates and amplitudes of the two phases were analyzed. Plotting the rate of the fast phase of the reaction versus [proR9] results in a straight line with a slope of 1.0×10^5 M^{-1} s^{-1} and intercept at 0.3 s^{-1} (Figure 4A). The amplitude of the fast phase increased as [proR9] increased and leveled off at 85% of the total fluorescence change at [proR9] > 20 μM (Figure 4B). The amplitude of the slow phase decreased with increasing [proR9] and leveled off at 15% at [proR9] > 20 μM (Figure 4B). The total amplitude change is independent of [proR9].

According to our model, the fast phase of the reaction corresponds to the formation of the initial collision complex PS_I (binding phase) and the slow phase corresponds to the decay of PS_I and formation of PS (isomerization phase). The slope from fitting the fast phase rate versus [proR9] would be the k_1, which is 1.0×10^5 M^{-1} s^{-1}. The rate of the slow phase of the reaction increased with [proR9] and leveled off at around 0.15 s^{-1} at [proR9] > 20 μM (Figure 4B).

Measuring the Accumulation of Folded Complex. A double-jump renaturation−denaturation experiment was designed to study the rate of accumulation of fully folded complex directly (*29*). In the first mixing step, 1.5 μM of unfolded subtilisin sbt15 or sbt70 is mixed with an excess amount of proR9 in the folding buffer 30 mM Tris and 5 mM KP_i, pH 7.5, at 25 °C. The folding mixture is aged for varied lengths of time. In the second mixing step, the aged mixture is denatured by mixing with phosphoric acid, with final pH 2.3. The rate of acid denaturation for the fully folded complex, PS, at pH 2.3 is much slower than the denaturation of PS_I. Thus, by measuring the fluorescence amplitude of acid denaturation as a function of the aging time of the folding reaction, we were able to monitor the accumulation of folded complex. The double jump data were plotted as fraction of PS versus folding time for sbt15 and sbt70. Figure 5 shows the rate of accumulation of PS as a function of folding time from an experiment in which 15 μM of proR9 and 1.5 μM of denatured sbt15 were present in the folding reaction. The kinetics were complex and could not be fit adequately with the two-step mechanism above. The simpliest mechanism which closely described the data includes two denatured forms of subtilisin, S_U and $S_{U'}$, which form the initial complex with proR9 (PS_I) at the same rate but which isomerize to the fully folded complex at much different

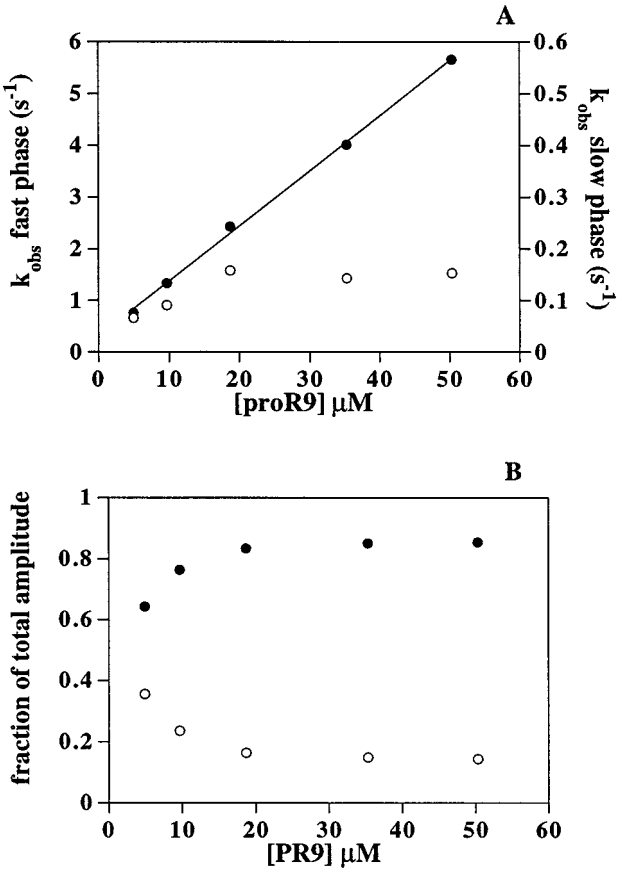

FIGURE 4: Plot of rates and amplitudes for folding of Sbt15 and proR9. Time courses for folding as followed by fluorescence (as shown in Figure 3) were fit to double exponential equations. The rates constants for the fast and slow phases plotted vs [proR9] are shown in part A. The amplitudes for the fast and slow phases plotted vs [proR9] are shown in part B.

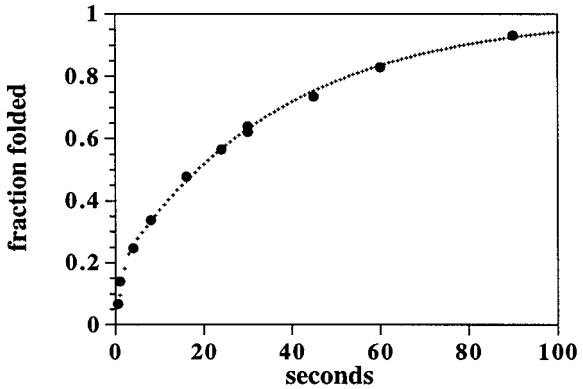

FIGURE 5: Plot of the accumulation of folded complex by double jump renaturation-denaturation. One micromolar denatured Sbt15 and 15 μM proR9 were returned to native conditions (30 mM Tris, pH 7.5, 25 °C) and allowed to fold for aging times from 0.5 to 90 s. In the second step the aged mixture is mixed with phosphoric acid bringing the sample to pH 2.3. The amplitude of the denaturation reaction is determined for each aging time to determine how much folded complex has accumulated. Solid circles show the accumulation of PS. Also shown is the KinTekSim simulation of PS as a function of folding time using the rate constants given in the text (small crosses).

rates. Accordingly, k_1 is assigned to the same value as $k_{1'}$ in the simulation. At the start of the simulation, 77% of the subtilisin is in the slow-folding S_U form and the remaining 23% is in the faster-folding $S_{U'}$ form. The fit with the

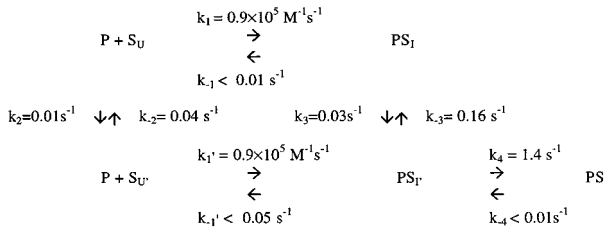

experimental data is more sensitive to changes in k_1, $k_{1'}$, k_3, k_{-3}, and k_4 than the other rate constants. Hence, k_{-1}, $k_{-1'}$, k_2, k_{-2}, and k_{-4} are not well determined by this experiment. This mechanism was tested using proR9 concentrations of 7.5, 11.25, 22.5, 30, and 37.5 μM. Folding kinetics at all [proR9] agree with the KinTekSim simulation curve using the same set of rate constants (data not shown). The model was also tested with subtilisin sbt70 and using 0.1 M KP_i, pH 7.0, 25 °C, as the folding condition. All results agree with the same basic mechanism, with slightly different sets of rate constants.

Folding Kinetics as a Function of Denaturation Time. To learn more about the multiple denatured forms of subtilisin, a double jump experiment was designed to study the effect of denaturation time on the rates and amplitudes of the folding reaction (*30*, *31*). In the first mixing reaction, 3 μM of subtilisin sbt15 is denatured by mixing with phosphoric acid, and the denaturation reaction is aged for varied lengths of time. The second mixing step returns the solution to pH 7.0 (final conditions 1 μM of sbt15 and 10 μM of proR9 in 0.1 M KP_i, pH 7.0, at 25 °C). The folding process is then followed by fluorescence change, and the rate and amplitude changes were determined. About 10 s of denaturation time is required before the amplitude of renaturation reaches its maximum value. This corresponds to the time required to unfold sbt15 under the acid conditions, as determined by fluorescence and CD changes (k_{unfold} = 0.47 s^{-1}, data not shown). After 10 s of denaturation, the refolding curves are clearly biphasic and were fitted with double exponential equations. The rate for the fast phase (k_1) is 1 s^{-1}, and the rate of the slow phase is 0.14 s^{-1}. These rates remain constant for all denaturation times longer than 10 s. Although the total amplitude changes remains constant after 10 s of denaturation, the amount of the total contributed by each phase varies as a function of denaturation time (Figure 6). The amplitude of the fast phase decreases at a rate of 0.06 s^{-1} before leveling out at about 80% of the total amplitude change, and the amplitude of the slow phase increases at a rate of 0.06 s^{-1} before leveling out at about 20% of the total amplitude change. These results indicate that denaturation occurs in two phases. We suspected that this was due to the isomerization of prolines in the unfolded state.

To confirm this interpretation of the denaturation behavior, the experiment was repeated using the subtilisin mutant sbt70. Sbt70 unfolds much faster in acid than sbt15. The unfolding rate of sbt70, as measured by fluorescence or CD, is 30 s^{-1} (data not shown). In the double jump denaturation-renaturation experiment, less than 0.5 s of denaturation of sbt70 is required for the maximum amplitude of renaturation to be observed. After denaturation times of ≥0.5 s, the

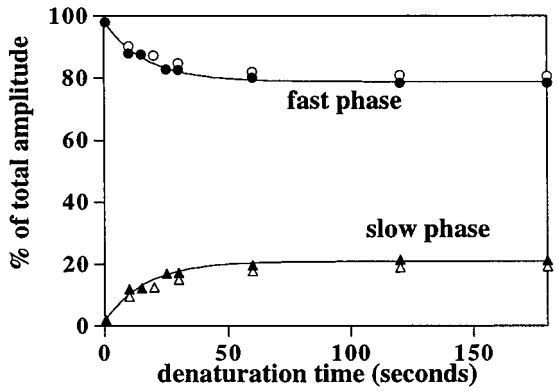

FIGURE 6: Measuring the rate of proline isomerization in the unfolded state by double jump denaturation renaturation. Sbt15 and Sbt70 were denatured in phosphoric acid for for times ranging 10−120 s for sbt15 and 0.5−120 s for sbt70. Samples were then renatured in 0.1M KP_i, pH 7.0 at 25 °C. The amplitudes of the fast and slow renaturation phases of the reaction are plotted as a function of denaturation time: (open circles) fast phase of sbt15; (solid circles) fast phase of sbt70; (open triangles) slow phase of sbt15; (solid triangles) slow phase of sbt70. Also shown is a single-exponential fit with a rate constant of 0.06 s^{-1}.

folding reactions were fit to double-exponential equations with the rate for the fast phase equal to 0.78 s^{-1} and the rate of the slow phase equal to 0.1 s^{-1}. These rates remain constant for all denaturation times longer than 0.5 s. The amount of the total amplitude contributed by the fast and slow renaturation phases varies as a function of denaturation time as shown in Figure 6. After 0.5 s of denaturation, the amplitude for the fast phase decreased at a rate of 0.06 s^{-1} and the amplitude for the slow phase increased at a rate of 0.06 s^{-1}.

Experiments with both sbt15 and sbt70 show that there are two steps in the denaturation process. The faster step occurs at the rate of global unfolding (0.47 s^{-1} for sbt15 and 30 s^{-1} for sbt70). The slower step is not associated with any spectral changes in subtilisin and occurs at a rate of 0.06 s^{-1} for both sbt15 and sbt70. These results suggest that the slow phase involves isomerization of prolyl peptide bonds in unfolded species (*30*). There are 13 proline residues in both subtilisin mutants. All but one (Pro168) exists as trans isomers in the native structure (*32*). The peptide bond between proline and its preceding amino acid (Xaa−Pro bonds) exist as a mixture of cis and trans isomers in solution unless structural constraints such as in folded proteins stabilize one of the two isomers. In the absence of ordered structure, the trans isomer is favored slightly over the cis isomer. The isomerization trans ⇔ cis is an intrinsically slow reaction with rates at 0.1−0.01 s^{-1} at 25 °C. Upon acid denaturation of subtilisin, the structural constraints are removed and the trans and cis isomers of all 13 prolyl peptide bonds gradually come to equilibrium in the unfolded state, resulting in 2^{13} different proline isomer combinations. The fact that the rate of the fast phase of the reaction remains constant as a function of denaturation time shows that the rate of the initial binding reaction of proR9 with unfolded subtilisin is not influenced by the isomerization state of prolines. The next section examines the much simpler senario in which catalyzed folding occurs from a denatured state in which all prolines are native-state isomers.

Measuring the Accumulation of Folded Complex at Short Denaturation Time. To study the catalyzed folding rate of

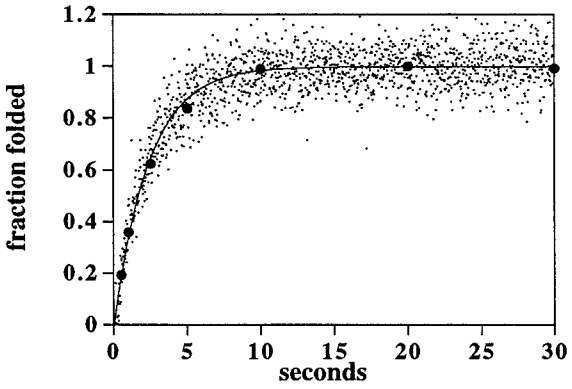

FIGURE 7: Folding kinetics of sbt70 after short denaturation time. Refolding kinetics of sbt70 were determined after 0.5 s of denaturation (small dots) using a double jump denaturation-renaturation procedure as described in the text. Also shown is the accumulation of PS after 0.5 s of denaturation (solid circles), as measured in a triple jump denaturation-renaturation−denaturation experiment.

subtilisin in the absence of prolyl peptide bond isomerization, folding kinetics were measured after a short denaturation time. Subtilisin sbt70 was used since the denaturation reaction is >98% complete in 0.5 s. The rapid denaturation time minimizes the amount of prolyl peptide bond isomerization occurring during the time require to unfold sbt70. After the 0.5 s denaturation step, the folding process was recorded as fluorescence increase versus time. The refolding condition was 30 mM Tris and 5 mM KP_i, pH 7.5, at 25 °C, with 0.5 μM of sbt70 and [proR9] = 5, 10, or 20 μM. At all three concentrations of proR9, folding kinetics are first order. At [proR9] = 5 μM, the observed folding rate is 0.4 s^{-1} (Figure 7). The observed rate of folding increases as concentration of proR9 increased and follows a linear relationship. The slope of the pseudo-first-order rate constants vs [proR9] yielded $k_{obs} = 9 \times 10^4$ M^{-1} s^{-1}.

To be confident that the fast kinetics observed above represents complete refolding to the native complex, we performed a triple mixing experiment to measure the accumulation of native complex directly. Sbt70 was denatured for 0.5 s in the first mixing step, then refolded with proR9 in 30 mM Tris and 5 mM KP_i, pH 7.5, at 25 °C for different aging times in the second mixing step. In the third mixing step, the folding reaction was denatured in phosphoric acid and the amplitude change of fluorescence was recorded as a function of refolding time. Figure 7 shows the results of the triple-jump experiment using 5 μM of proR9. The fraction of folded complex is plotted versus time of renaturation. Also shown is a parallel double jump experiment in which the fluorescence change is recorded during folding in 30 mM Tris and 5 mM KP_i, pH 7.5. Both sets of data can be fit to a single-exponential equation with a rate constant of 0.4 s^{-1}. This demonstrates that by denaturating sbt70 for just long enough time that unfolding was complete but prolyl peptide bond isomerization was negligible, the folding of the denatured subtilisin followed fast single-exponential kinetics. No intermediate was detectible in the course of the reaction because the formation of PS from PS_I is faster than the formation of initial collision complex PS_I from P and S_U. The mechanism of folding reaction for fast-folding denatured subtilisin sbt70 is as follows:

$$P + S_U \underset{<0.05\ s^{-1}}{\overset{9 \times 10^4\ M^{-1}\ s^{-1}}{\rightleftharpoons}} PS_I \underset{<0.01\ s^{-1}}{\overset{>3\ s^{-1}}{\rightleftharpoons}} PS$$

where S_U is denatured subtilisin sbt70 with all prolyl peptide bond isomers the same as in the native structure. According to the mechanism proposed above, the pseudo-first-order rate constant would reach its maximum when [proR9] is high enough that the value k_1 [proR9] > ($k_2 + k_{-2}$). That point has not been reached at [proR9] = 20 μM. From running simulations of the two-step mechanism above with $k_1 = 9 \times 10^4$ M^{-1} s^{-1} and $k_{-1} < 0.05$ s^{-1}, however, we can determine that $k_2 + k_{-2} > 3$ s^{-1}. If $k_2 + k_{-2}$ were smaller than 3 s^{-1}, we would have detected a lag phase in the accumulation of the folded complex SP.

DISCUSSION

Experimental Synopsis. In this paper, the stabilized pro-domain mutant proR9 was used to study the transient-state kinetics of the pro-domain-catalyzed folding reaction to address the following questions: why does subtilisin fold slowly without the pro-domain and what does the pro-domain do to accelerate the folding rate? There are three central findings.

(1) ProR9 folds subtilisin much faster than the predominantly unfolded proWT. The folding reaction with proR9, as well as five stabilized pro-domain mutants described earlier (*19*), show a correlation between the stability of the pro-domain and its ability to accelerate subtilisin folding.

(2) At micromolar concentrations of proR9, the subtilisin-folding reaction becomes limited by the rate at which prolines in the unfolded state can isomerize to their native conformation. The results of experiments measuring the accumulation of PS after a long denaturation time showed that renaturation kinetics could be modeled reasonably well using only two denatured species which form the initial complex with proR9 (PS_I) at the same rate but which isomerize to the fully folded complex at much different rates. In this model, 77% of the subtilisin isomerizes to the native form slowly and the remaining 23% isomerizes at a rate of 1.5 s^{-1}. This suggests that the slow-folding 77% may be unfolded subtilisin with the trans form of proline 168, which must isomerize to the cis form during refolding. The cis to trans isomerizations of other prolines would seem to occur relatively quickly in the proR9-catalyzed reaction. A realistic mechanism would involve 2^{13} prolines isomer combinations in unfolded subtilisin, each folding with different kinetics. Even though the realistic model would be hopelessly complex, a simple kinetic model with only two denatured species is robust enough to predict folding behavior at different [proR9]. It should be understood, however, that individual rate constants for many different proline isomer combinations are blended together into just two sets of rate constants in the simple mechanism.

(3) In the absence of proline isomerization, the rate of subtilisin folding is rapid and at [proR9] ≤ 20 μM is limited by the rate at which the proR9 forms a collision complex with unfolded subtilisin. The rate of the isomerization of the collision complex, PS_I, to the folded complex, PS is >3 s^{-1}. The observed second-order rate constant for subtilisin folding is $\sim 10^5$ M^{-1} s^{-1}, the same as the rate of just the binding phase when proline isomerization is limiting. By comparison, the rate of proR9 binding to folded subtilisin is about 10^6 M^{-1} s^{-1}.

Why Is Uncatalyzed Subtilisin Folding Slow? In the presence of micromolar concentrations of proR9, the rate of subtilisin folding into a complex with proR9 becomes typical of in vitro folding rates for many small globular proteins. That is, independent of proline isomerization, folding is largely complete within a few seconds (*30*). The question remains as to why subtilisin folding is so slow without the pro-domain. With calcium-free subtilisin, the problem is not that the native state is unstable relative to the intermediate or the other unfolded states, as has been proposed for α-lytic protease (*33*). Our argument has been that uncatalyzed folding of subtilisin is slow because of the low stability of intermediates (*9*, *17*, *19*). An efficient folding pathway implies that productive intermediates are significantly more stable than the surrounding landscape of unfolded and misfolded conformations. Native folding intermediates of mature subtilisin may have similar or lower stability than unfolded or misfolded states. This would result in a large entropic barrier to folding, since most of the native structure would have to be formed before a significant free-energy well is reached in conformational space (*34*). This is surprising since a folding pathway seems to be a consequence of a stable native state for many proteins. Native-state H−D exchange experiments for several proteins have shown that partially folded states exist with significantly lower energy than the globally unfolded state (*35*−*37*). These partially folded states are important intermediates in the folding pathway of these proteins. In the case of a broad specificity proteinase such as subtilisin, however, there is likely a selection against stable intermediate states. Assuming that partially folded intermediates are good substrates for autolysis, the half-life of active subtilisin would be determined by the equilibrium between the proteinase-resistant native state and the lowest energy, proteinase-labile intermediate. Thus to avoid autolysis, partially folded conformations must be of much higher energy than the native state so that excursions between the two states are rare. This presents a folding problem for a single domain protein of the size of subtilisin, however, because most of the tertiary structure must be acquired before a free-energy well is encountered in conformational space. The enormous loss of conformational entropy before that energy well occurs would result in a large transition state barrier to folding. In this model, the transition state is of high energy because of its low confomational entropy, not because unfavorable protein−protein or protein−solvent rearrangements are required in folding. The temperature dependence of the catalyzed folding reaction is consistent with this model. The maximum rate of catalyzed folding occurs at 25 °C, at which point the activation enthaply of the folding reaction is zero and the activation barrier is entirely entropic (*7*). The pro-domain decreases the entropic barrier by stabilizing the intermediate, S_I, and pushing the transition state back toward a less folded form of subtilisin. Thus, much less conformational entropy is lost in the transition state. Once over the barrier, folding of PS_I to PS is rapid (except for proline isomerization).

In order for wild-type subtilisin to be resistant to autoproteolysis, a large barrier must be created between the native state and any partially folded states after folding is completed. For active subtilisin, this energetic barrier is created by the proteolysis of the pro-domain. Once folding to the complex, SP, has been achieved, the lowest energy intermediate becomes the dissociated species, P+S. Dissociation of the complex results in proteolysis of the pro-domain, leaving a large barrier between native subtilisin and other intermediate states. This model would predict that native state H−D exchange studies on subtilisin would not detect intermediates with significantly lower energy than the globaly unfolded state. These experiments are in progress.

ACKNOWLEDGMENT

The authors wish to thank Richard Prescott for synthesizing the oligonucleotides used in site-directed mutagenesis and DNA sequencing and Patrick Alexander, Susan Strausberg, and Michael Gilson for useful discussion.

REFERENCES

1. Wells, J. A., Ferrari, E., Henner, D. J., Estell, D. A., and Chen, E. Y. (1983) *Nucleic Acids Res. 11*, 7911−7925.
2. Vasantha, N., Thompson, L. D., Rhodes, C., Banner, C., Nagle, J., and Filpula, D. (1984) *J. Bacteriol. 159*, 811−819.
3. Wong, S., and Doi, R. (1986) *J. Biol. Chem. 261*, 10176−10181.
4. Power, S. D., Adams, R. M., and Wells, J. A. (1986) *Proc. Natl. Acad. Sci. U.S.A.* 83, 3096−3100.
5. Ikemura, H., Takagi, H., and Inouye, M. (1987) *J. Biol. Chem. 262*, 7859−7864.
6. Bryan, P., Alexander, P., Strausberg, S., Schwarz, F., Wang, L., Gilliland, G., and Gallagher, D. T. (1992) *Biochemistry 31*, 4937−4945.
7. Strausberg, S., Alexander, P., Wang, L., Schwarz, F., and Bryan, P. (1993) *Biochemistry 32*, 8112−8119.
8. Gallagher, T. D., Gilliland, G., Wang, L., and Bryan, P. (1995) *Structure 3*, 907−914.
9. Bryan, P., Wang, L., Hoskins, J., Ruvinov, S., Strausberg, S., Alexander, P., Almog, O., Gilliland, G., and Gallagher, T. D. (1995) *Biochemistry 34*, 10310−10318.
10. Baker, D., Silen, J., and Agard, D. (1992) *Proteins: Struct., Funct., Genet. 12*, 339−344.
11. Baker, D., Sohl, J., and Agard, D. A. (1992) *Nature 356*, 263−265.
12. Winther, J. R., and Sorensen, P. (1991) *Proc. Natl. Acad. Sci. U.S.A. 88*, 9330−9334.
13. Cawley, N. X., Olsen, V., Zhang, C. F., Chen, H. C., Tan, M., and Loh, Y. P. (1998) *J. Biol. Chem. 273*, 584−591.
14. van den Hazel, H. B., Kielland-Brandt, M. C., and Winther, J. R. (1993) *J. Biol. Chem. 268*, 18002−18007.
15. Vernet, T., Berti, P. J., de Montigny, C., Musil, R., Tessier, D. C., Menard, R., Magny, M. C., Storer, A. C., and Thomas, D. Y. (1995) *J Biol Chem 270*, 10838−10846.
16. Steiner, D., Smeekens, S. P., Ohagi, S., and Chan, S. J. (1992) *J. Mol. Biol. 267*, 23435−23438.
17. Wang, L., Ruvinov, S., Strausberg, S., Gallagher, T. D., Gilliland, G., and Bryan, P. (1995) *Biochemistry 34*, 15415−15420.
18. Ruvinov, S., Wang, L., Ruan, B., Almog, O., Gilliland, G., Eisenstein, E., and Bryan, P. (1997) *Biochemistry 36*, 10414−10421.
19. Wang, L., Ruan, B., Ruvinov, S., and Bryan, P. N. (1998) *Biochemistry 37*, 3165−3171.
20. Alexander, P., Fahnestock, S., Lee, T., Orban, J., and Bryan, P. (1992) *Biochemistry 31*, 3597−3603.
21. Studier, F. W., and Moffatt, B. A. (1986) *J. Mol. Biol. 189*, 113−130.
22. Johnson, B. H., and Hecht, M. H. (1994) *Biotechnology 12*, 1357−60.
23. Barshop, B. A., Wrenn, R. F., and Frieden, C. (1983) *Anal. Biochem. 130*, 134−145.
24. Zimmerle, C. T., and Frieden, C. (1989) *Biochem. J. 258*, 381−387.
25. Ruan, B., Hoskins, J., Wang, L., and Bryan, P. N. (1998) *Protein Sci. 7*, 2345−2353.

26. Eder, J., Rheinnecker, M., and Fersht, A. R. (1993) *J. Mol. Biol. 233*, 293−304.
27. Bryan, P. N. (1995) in *Intramolecular chaperones and protein folding* (Shinde, U., and Inouye, M., Eds.) pp 85−112, R. G. Landes, Austin.
28. Johnson, K. A. (1992) *Enzymes 20*, 1−61.
29. Kiefhaber, T. (1995) *Proc. Natl. Acad. Sci. U.S.A. 92*, 9029−9033.
30. Brandts, J. F., Halvorson, H. R., and Brennan, M. (1975) *Biochemistry 14*, 4953−4963.
31. Kiefhaber, T., and Schmid, F. X. (1992) *J. Mol. Biol. 224*, 231−240.
32. McPhalen, C. A., and James, M. N. G. (1988) *Biochemistry 27*, 6582−6598.
33. Sohl, J. L., Jaswal, S. S., and Agard, D. A. (1998) *Nature 395*, 817−819.
34. Levinthal, C. (1968) *J. Chim. Phys. 65*, 44−45.
35. Bai, Y., Sosnick, T. R., Mayne, L., and Englander, S. W. (1995) *Science 269*, 192−197.
36. Chamberlain, A. K., Handel, T. M., and Marqusee, S. (1996) *Nat. Struct. Biol. 3*, 782−787.
37. Chung, E. W., Nettleton, E. J., Morgan, C. J., Gross, M., Miranker, A., Radford, S. E., Dobson, C. M., and Robinson, C. V. (1997) *Protein Sci. 6*, 1316−1324.
38. Kraulis, P. J. (1991) *J. Appl. Crystallogr. 24*, 946−950.

BI990362N